

Effect of different types of nano-size oxide particulates on microstructural and mechanical properties of elemental Mg

S. F. HASSAN, M. GUPTA

Department of Mechanical Engineering, National University of Singapore, 9 Engineering Drive 1, Singapore, 117576

E-mail: mpegm@nvs.edu.sg

Published online: 3 March 2006

In the present study, magnesium based composites were fabricated with three different types of 1.1 volume percent nanosize oxide particulate reinforcements (i.e., Al_2O_3 , Y_2O_3 and ZrO_2) using blend-press-sinter methodology avoiding ball milling. Microstructural characterization of the materials revealed reasonably uniform distribution of nano-reinforcement, significant grain refinement and the presence of minimal porosity. Mechanical properties characterization revealed that the incorporation of nano-sized oxide particulates as reinforcement led to a simultaneous increase in hardness, 0.2% yield strength, UTS and ductility of pure magnesium. The results further revealed that the 0.2% yield strength, UTS and ductility combination of the magnesium containing nano-size Al_2O_3 remained higher when compared to high strength magnesium alloy AZ91 reinforced with much higher amount of micron size SiC particulates. An attempt is made in the present study to correlate the effect of different types of nano-sized oxide particulates on the microstructural and mechanical properties of magnesium.

© 2006 Springer Science + Business Media, Inc.

1. Introduction

Magnesium has history of technical use of more than 75 years [1] which diversified from automobile, aerospace to consumer electronics in recent days [2]. Simultaneous benefit of environmental protection and preservation of limited fossil fuel reserve by reducing weight of vehicles is the impetus in recent days in increasing interest of magnesium use by automobile producers. Magnesium based materials, which are the lightest metallic materials (1.74 g/cm^3 , which is about two-thirds of the density of aluminum and one-quarter of that of iron) offer many possibilities for weight reduction and most car producers are going to use 40–100 kg of magnesium based materials in near future [2–6]. Regulations on electromagnetic radiation limit turned consumer electronics (like mobile phone, notebook and camera) producers to use magnesium due its good resistance to electromagnetic radiation [2]. Intrinsic limited ductility of magnesium [7], which worsen further both in traditional alloys and reinforced composites [8–15] and adversely affect the most needed solid state formability of structural intricate parts, remains one of the major concern in its fabrication and application in recent days. However, some reports on simultane-

ous enhancement of strength and ductility of magnesium due to the presence of metastable finer precipitation [16, 17] and reinforcements [15, 18–20] and grain refinement [21] provides the impetus to the selection of thermally stable nano-size oxide ceramics particulates, i.e., Al_2O_3 , Y_2O_3 , and ZrO_2 , capable of forming chemical bond at the metal-reinforcement interface [22, 23]. The result of literature search indicates that only one attempt [15] is made to study the potential of development of magnesium based composites containing nano-size particulates such as Al_2O_3 and ZrO_2 using mechanical alloying technique. However, no attempt is made so far to synthesize the Mg based nano composites containing Al_2O_3 , Y_2O_3 , or ZrO_2 particulates using a simpler blend-press-sinter approach and to study the effect of types of oxide ceramics on the microstructural and mechanical properties of pure magnesium.

Accordingly, the primary aim of the present study was to synthesize magnesium based composite materials containing nano-size Al_2O_3 , Y_2O_3 , and ZrO_2 particulates, using blend-press-sinter powder metallurgy technique. The composites thus obtained were hot extruded and characterized for their microstructural and

mechanical properties. Particular emphasis was placed to study the effect of the presence of different types of particulates in nanolength scale on the microstructure and mechanical response of commercially pure magnesium.

2. Experimental procedures

2.1. Materials

In this study, magnesium particulates with size range of 60–300 μm of $\geq 98.5\%$ purity (supplied by Merck, Germany) were reinforced with 1.1 volume percentage of three different types of nano-size oxide ceramics. Al_2O_3 (average size of 50-nm) (supplied by Baikowski, Japan), Y_2O_3 (average size of 29-nm) and ZrO_2 (average size of 29–68-nm) (supplied by Nanostructured & Amorphous Materials Inc., USA) were used as reinforcements.

2.2. Primary processing

Blend-press-sinter type powder metallurgy technique was used to synthesize all the composites. Preweighed metal and ceramic powder were mixed in a V-blender at 50-rpm for 6-h and were subsequently compacted to preforms (40 mm height with 36 mm diameter) using a 150-ton press. The preforms were coated with colloidal graphite and sintered in tube furnace at 500°C for 2-h under argon atmosphere. The synthesis of monolithic magnesium was carried out using similar steps except that no reinforcement particulates were added.

2.3. Secondary processing

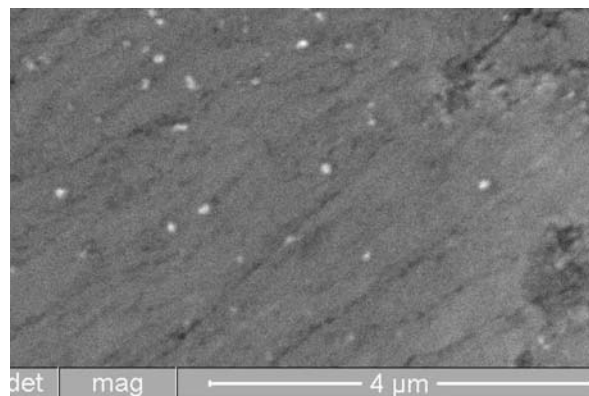
The sintered monolithic and composites preforms were hot extruded using an extrusion ratio of 20.25:1 on a 150 ton hydraulic press. Extrusion was carried out at 250°C. The preforms were held at 300°C for 90 min in a constant temperature furnace before extrusion. Colloidal graphite was used as lubricant. Rods of 8 mm diameter were obtained following extrusion.

2.4. Density measurement

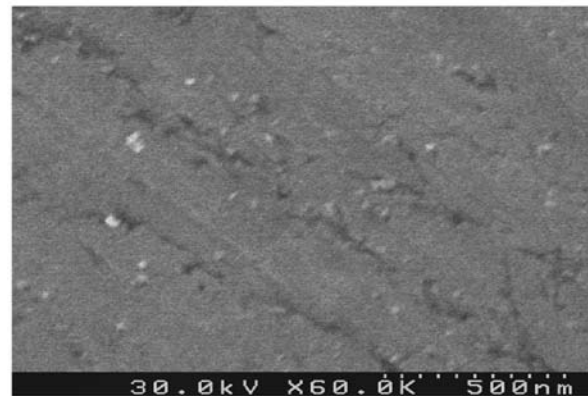
Density (ρ) measurements were performed in accordance with Archimedes' principle [11, 12] on three randomly selected polished samples of Mg, Mg/ Al_2O_3 , Mg/ Y_2O_3 and Mg/ ZrO_2 taken from the extruded rods. Distilled water was used as the immersion fluid. The samples were weighed using an A&D ER-182A electronic balance, with an accuracy of ± 0.0001 g. Theoretical densities of materials were calculated assuming they are fully-dense and there is no reinforcement/matrix interfacial reaction to measure the volume percentage of porosity in the end materials. Rule-of-Mixture was used in both of the calculations.

2.5. Microstructural characterization

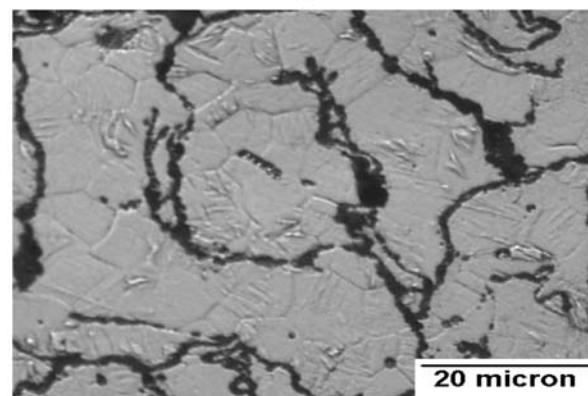
Microstructural characterization studies were conducted on metallographically polished extruded samples to investigate reinforcement distribution, interfacial integrity between the matrix and reinforcement, and morphological characteristics of grains. The OLYMPUS metallographic microscope, Hitachi S4100 Field-Emission Scanning Electron Microscope (FESEM) and Philips Dual Beam Scanning Electron Microscope (Quanta 3D) were used.



(a)



(b)



(c)

Figure 1 Representative micrographs showing: (a) and (b) reinforcement distribution of Al_2O_3 and ZrO_2 , and (c) typical grain morphology in the case of Mg/ ZrO_2 , respectively.

Image analysis using the Scion system was carried out to determine the grain size of the materials.

2.6. Hardness

Microhardness and macrohardness measurements were made on the polished Mg and composites samples. Vickers microhardness was measured by Matsuzawa MXT50 automatic digital microhardness tester using 25gf-indenting load. Rockwell 15T superficial scale was used for macrohardness measurement in accordance with ASTM E18-94 standard.

2.7. Tensile testing

The smooth bar tensile properties of the extruded Mg and composites samples were determined in accordance with ASTM test method E8M-01 using Instron 8516 machine with a crosshead speed set at 0.254 mm/min on round tension test specimens of 5 mm diameter and 25 mm gauge length. Instron 2630–100 Series Clip-On type extensometer was used for strain recording. Fractography was done on the tensile fractured samples using JEOL JSM-5800 LV Scanning Electron Microscope (SEM).

3. Results

3.1. Macrostructural characteristics

The result of macrostructural characterization of preforms and extruded rods of Mg and composites did not reveal any macrostructural defects. The results of density measurement show that near dense composites are formed (see Table I).

3.2. Microstructural characteristics

Microstructural studies conducted on the extruded composites specimens showed reasonably uniform reinforcement particulate distribution (see Fig. 1a and b), good particulates-matrix interfacial integrity in terms of debonded regions and the presence of minimal porosity. Results of grain size measurements revealed that all the composite samples exhibited significantly lower grain size when compared to pure magnesium (see Table I).

3.3. Hardness

The results of the macrohardness and microhardness measurements conducted on extruded Mg and composites samples revealed an increase in matrix hardness (both at macro and micro level) with the presence of nano-size reinforcements (see Table II). Both macrohardness and microhardness values reach highest in the case of Mg/Al₂O₃ composites.

3.4. Tensile characteristics

Results of ambient temperature tensile tests revealed significant improvement in 0.2%YS, UTS, and ductility (see Tables II and III) of magnesium with the addition of nano-size oxide particulates. However, overall combination of tensile properties remains highest in the case of Mg/Al₂O₃ composite. Fracture behavior of the matrix was changed from brittle for pure Mg to near ductile in the case of composites (see Figs 2 and 3).

4. Discussion

4.1. Microstructural characteristics

Microstructural characterization of extruded composites samples are discussed in terms of: (a) distribution of reinforcement, (b) reinforcement-matrix interfacial characteristics, (c) grain size and shape, and (d) amount of porosity.

The reasonably uniform distribution of reinforcement particulates (see Fig. 1a and b) can be attributed to: (a) suitable blending parameters and (b) high extrusion ratio used in secondary processing. Theoretically, when secondary processing with a large enough deformation is introduced, homogeneous distribution of reinforcements can be achieved regardless of the size difference between matrix powder and reinforcement particulates [24]. Almost zero standard deviation in density measurement results (see Table I) also reflect the uniform distribution of the reinforcement in processed materials. Interfacial integrity between matrix and reinforcement was assessed in terms of interfacial debonding and microvoids at the particulate-matrix interface and was found to be good as expected from metal/oxide systems [22]. Good interfacial integrity may further be attributed to the tendency of reaction between matrix/reinforcement in the processed composites [23]. To investigate the degree of magnesium-reinforcement reaction, controlled studies were carried out on the identically processed composites each with 10-vol% of reinforcement using XRD technique. Samples were exposed to CuK α radiation ($\lambda = 1.5418 \text{ \AA}$) with a scan speed of 0.5 deg/min on an automated Shimadzu LAB-X XRD-7000 diffractometer. Results revealed absence of any reaction phase indicating that reaction whatsoever was not detectably promoted in the processing methodology used in the present study.

Metallography of the extruded samples revealed that the matrix recrystallized completely. The sizes of the near-equiaxed grains of magnesium matrix in the case of composite samples were distinctly smaller when compared to that of unreinforced magnesium (see Table I). Grain refinement in the case of composite samples can primarily be attributed to the coupled effects of: (i) capability of fine second phase particulates to nucleate magnesium grains during recrystallization, and (ii) restricted growth of recrystallized magnesium grains as a result of pinning by the presence of finer reinforcement particulates. The fundamental principles behind the ability of inclusions

TABLE I Results of density, porosity and grain morphology of Mg and composites

| Materials | Reinforcement (wt%) | Density (gm/cm ³) | | | Grain characteristics | |
|--------------------------------------|---------------------|-------------------------------|---------------------|--------------|------------------------|---------------|
| | | Theoretical | Experimental | Porosity (%) | Size (μm) | Aspect ratio |
| Mg | 0.0 | 1.7400 | 1.7387 \pm 0.0022 | 0.08 | 60 \pm 10 | 1.6 \pm 0.3 |
| Mg/1.1Al ₂ O ₃ | 2.5 | 1.7647 | 1.7632 \pm 0.0048 | 0.09 | 31 \pm 13 | 2.2 \pm 1.3 |
| Mg/1.1Y ₂ O ₃ | 3.1 | 1.7763 | 1.7675 \pm 0.0046 | 0.49 | 12 \pm 3 | 1.6 \pm 0.4 |
| Mg/1.1ZrO ₂ | 3.7 | 1.7861 | 1.7829 \pm 0.0006 | 0.18 | 11 \pm 3 | 1.5 \pm 0.2 |

TABLE II Room temperature mechanical properties of Mg and composites samples.

| Materials | Hardness | | 0.2% YS (MPa) | UTS (MPa) | Ductility (%) |
|--------------------------------------|----------------|----------------|---------------|-------------|----------------|
| | Macro (15HRT) | Micro (HV) | | | |
| Mg | 43.5 \pm 0.3 | 37.4 \pm 0.4 | 132 \pm 7 | 193 \pm 2 | 4.2 \pm 0.1 |
| Mg/1.1Al ₂ O ₃ | 59.7 \pm 0.5 | 69.5 \pm 0.5 | 194 \pm 5 | 250 \pm 3 | 6.9 \pm 1.0 |
| Mg/1.1Y ₂ O ₃ | 49.0 \pm 0.5 | 51.0 \pm 0.7 | 153 \pm 3 | 195 \pm 2 | 9.1 \pm 0.2 |
| Mg/1.1ZrO ₂ | 48.4 \pm 0.7 | 45.7 \pm 0.6 | 146 \pm 1 | 199 \pm 5 | 10.8 \pm 1.3 |
| AZ91/9.4SiCP[8] | | | 191 | 236 | 2 |

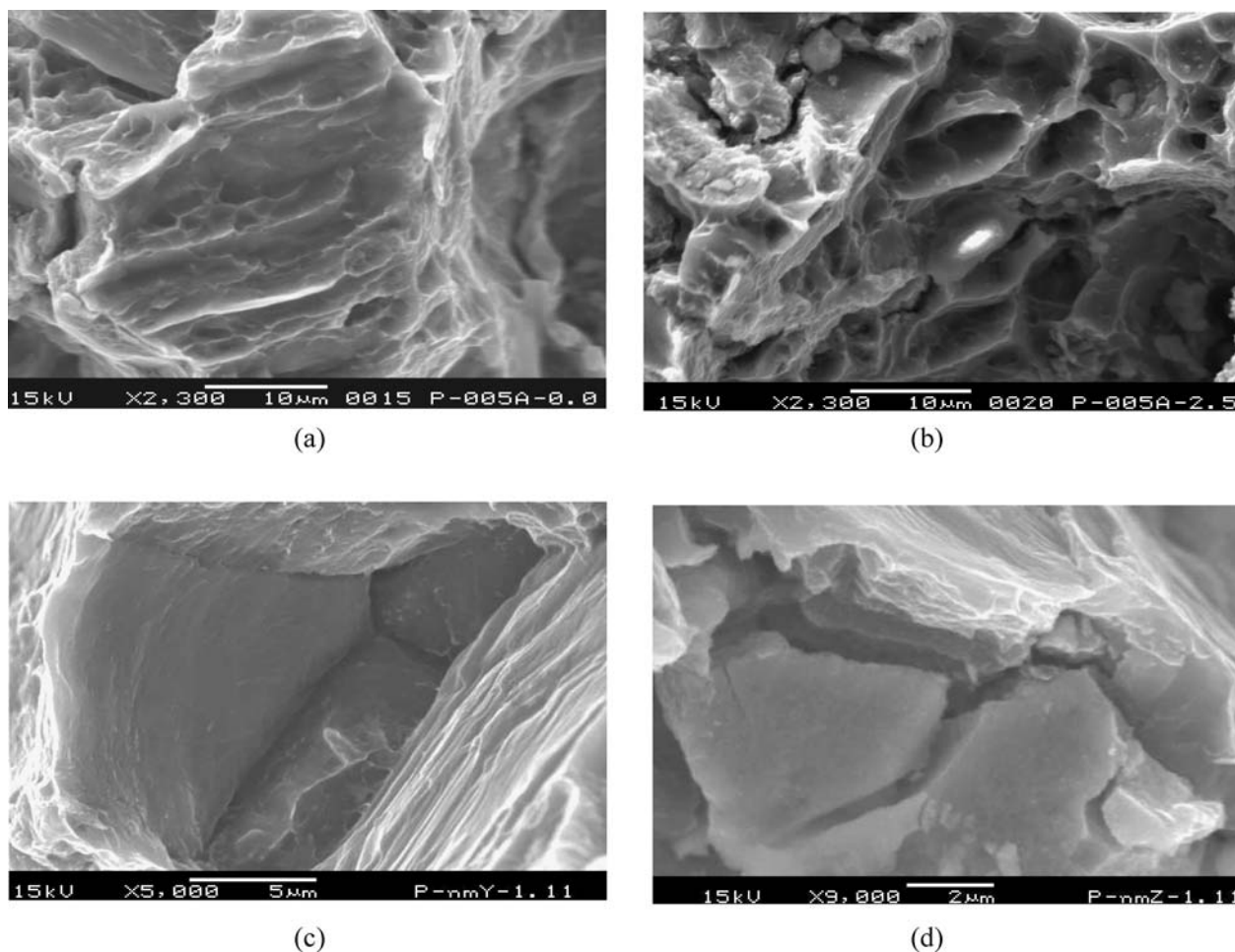
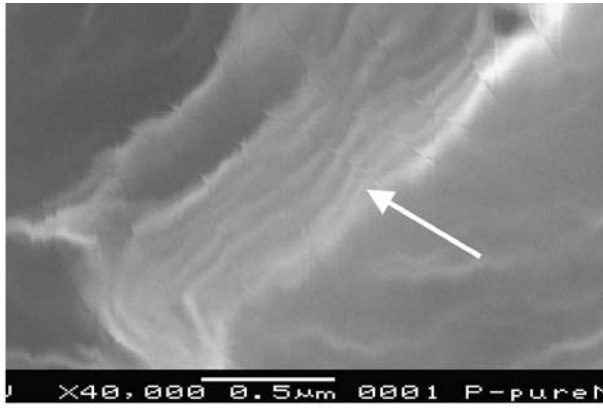


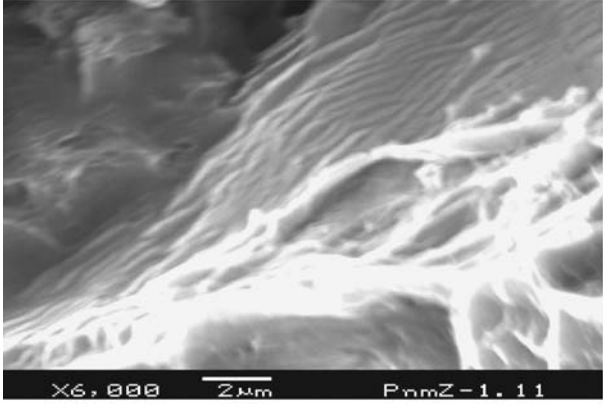
Figure 2 Representative SEM fractographs showing: (a) cleavage steps in Mg, (b) dimples in Mg/Al₂O₃, (c) intergranular crack propagation in Mg/Y₂O₃, and (d) branching of propagating crack at reinforcement in Mg/ZrO₂, respectively.

in the metallic-matrix to nucleate recrystallized grains [25] and to inhibit grain growth [7] have been already established and will not be discussed here. However, the result of grain size measurement revealed Y₂O₃ and ZrO₂

particulates to be more effective than Al₂O₃ particulates in grain boundary pinning and the plausible reason might be their higher thermal stability in magnesium [15, 22, 23, 26].



(a)



(b)

Figure 3 Representative SEM fractographs showing: (a) straight lines (marked by arrows) due to slip in the basal plane in the case of pure Mg, and (b) uneven lines due to combined effect of basal and non-basal slip in the case of Mg/ZrO₂, respectively.

The presence of minimal porosity in composite materials, also supported by the experimental density values (see Table I), can be attributed to the good compatibility between oxide ceramic and Mg system [22] and appropriate selection of compaction, sintering and extrusion parameters [8, 27].

4.2. Mechanical behavior

The results of hardness measurements revealed that addition of nano-size reinforcement leads to a significant increase in both the macrohardness and microhardness (see Table II) of Mg and can be attributed primarily to: (a) the presence of relatively harder ceramic particulates in the matrix [10, 15], (b) a higher constraint to the localized matrix deformation during indentation due to their presence, and (c) reduced grain size (see Table I) [28, 29].

The results of room temperature tensile testing revealed significant increase in 0.2%YS and UTS (see Table II) of pure magnesium due to the presence of nano-size oxides as reinforcement and can primarily be attributed to the coupled effect of: (a) increase in grain

boundary area due to grain refinement [7, 28], (b) heavily built multi-directional thermal stress at the particulate/matrix interface at grain boundaries induced due to the large difference of coefficient of thermal expansion between matrix and reinforcement (CTE of Mg is $27.1 \times 10^{-6}/^{\circ}\text{K}$ [30], and Al₂O₃ is $7.4 \times 10^{-6}/^{\circ}\text{K}$, and ZrO₂ is $11.0 \times 10^{-6}/^{\circ}\text{K}$ [31], and Y₂O₃ is $7.5 \times 10^{-6}/^{\circ}\text{K}$ [32], respectively), and (c) the effective transfer of applied tensile load to the uniformly distributed well-bonded strong oxides particulates (yield strength of ceramic materials lies much higher than metallic materials [33]) [11, 12, 34]. In general, the yield stress of material is the stress required to operate dislocation sources and is governed by the dislocation density and magnitude of all the obstacles that restrict the motion of dislocation in the matrix. Under the applied stress, enormous number of reinforcement particulates and increasing amount of grain boundaries (due to significant grain refinement) acts as obstacles to the dislocation movement and end up with dislocation pile ups [18, 28]. Again, multi-directional thermal stress induced during processing easily starts multi-gliding system [35] under applied stress so that dislocations were found developing and moving in several directions. Multi-glide planes agglomerate under thermal and/or applied tensile stress to form grain boundary ledges [28]. As the applied tensile load increases, these ledges too act as obstacle to dislocation movement resulting in further pile-ups. The coupled effects of these obstacles lead to the significant increase in the yield strength of the composites over pure magnesium. However, increase in 0.2%YS and UTS of magnesium (see Table II) was found to be highest in the case of Mg/Al₂O₃ and lowest in the case of Mg/ZrO₂ composite and it can be attributed to the matrix/reinforcement interfacial compatibility governed stability. Al₂O₃ is most susceptible to diffusion controlled superficial reaction with magnesium [15, 22, 23, 36] to form strong interfacial bonding and that might be the reason of its highest strengthening effect on matrix material. Strengthening effect of finer Al₂O₃ particulates on metals like aluminum, copper and nickel has been reported much earlier [37].

It may very interestingly be noted that that yield strength of the composites irrespective of the particulate type exhibited a linear relationship with both microhardness and macrohardness of the composite materials and the variations are plotted as shown in Fig. 4. A curve fit, between hardness and yield strength ($\sigma_{0.2\%YS}$), can be represented as follows:

$$\sigma_{0.2\%YS} = 1.950 (\text{HV}) + 57.019; r^2 = 0.9914 \quad (1)$$

$$\sigma_{0.2\%YS} = 3.887 (\text{MH}) - 38.686; r^2 = 0.9923 \quad (2)$$

where, HV is microhardness, MH is macrohardness and r is the statistical coefficient indicative of the degree of curve fit obtained from the experimental data points, respectively. A value of $r = 1$ is indicative of

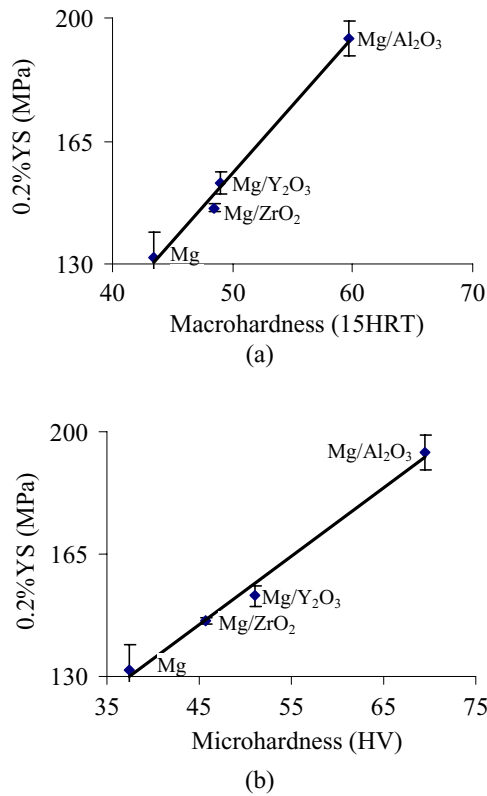


Figure 4 Graphical representation showing relation between: 0.2%YS and (a) macrohardness and (b) microhardness of Mg and composites.

perfect curve fit. Test results reveal the existence of a linear relationship between both the matrix hardness (macro and micro) and 0.2%YS due to the addition of different types of nanosize oxide reinforcements. In essence, the results of the hardness (macro and micro) measurements and tensile tests reveal that the magnitude of hardness and yield strength is dependent on the mutually interactive influences of the resistance offered to the motion of dislocations, and the plastic deformation capability of the metal matrix. Additional research efforts are currently being undertaken so as to establish a mathematical relationship for metal-matrix composites for magnesium matrix and different types of nanosize oxide reinforcement combinations. In related studies investigators have proposed such relationships in the case of monolithic materials [38, 39] and composite materials [40, 41]. The results clearly reveal that such relationship do exist for the nanocomposites such as those investigated in the present study.

Room temperature tensile test also revealed the capability of nano-size oxide particulates reinforcement to increase the ductility of pure magnesium. The increment in ductility of magnesium matrix due to presence of nano particulates can primarily be attributed to the coupled effect of: (a) grain refinement [21], (b) presence of reasonably uniformly distributed reinforcement particulates [18], and (c) slip on extra non-basal slip system [19]. Grain refinement particularly benefits hexagonal metals

TABLE III Specific strength and work of fracture of Mg and composites samples.

| Materials | Work of fracture | | |
|--------------------------------------|----------------------------------|-------------------------|---------------------|
| | (J/m ³) ^a | $\sigma_{0.2\%YS}/\rho$ | σ_{UTS}/ρ |
| Mg | 7.1 ± 0.3 | 76 | 111 |
| Mg/1.1Al ₂ O ₃ | 15.5 ± 2.6 | 110 | 142 |
| Mg/1.1Y ₂ O ₃ | 25.0 ± 3.3 | 103 | 134 |
| Mg/1.1ZrO ₂ | 34.7 ± 0.8 | 97 | 129 |
| AZ91/9.4SiCP [8] | | 102 ^b | 126 ^b |

^a Determined from engineering stress-strain diagram using EXCEL software.

^b Theoretical density is 1.8782 gm/cm³ assuming zero porosity.

in ductility increment where intergranular fracture arises from intercrystalline stresses [21] and this can be clearly seen in Fig. 2c. Again, dispersed phases in brittle matrix, where dislocation mobility is restricted and crack generation is relatively easy, act as ductility enhancer, an anomaly to their effect in ductile matrix [18]. Dispersed reinforcement particulates in brittle metal matrix serve to: (i) provides sites where cleavage cracks may open ahead of an advancing crack front, (ii) dissipate the stress concentration which would otherwise exist at the crack front (see Fig. 2d), and (iii) alter the local effective state of stress from plane strain to one of plane stress in the neighborhood of the crack tip. In addition, it has been understood through recent studies that non-basal slip system activate under axial tensile stress and increases ductility [19] which is also evident in fractography results obtained in this study (see Fig. 3). It is interesting to note that metallic particulate reinforcement like Ti [17, 18] and nano-size oxide dispersoids like Al₂O₃, Y₂O₃ and ZrO₂ in this study seems to be capable to activate non-basal slip system at room temperature in pure magnesium matrix and increases the ductility. However, ZrO₂ as reinforcement led to the highest increment in magnesium matrix among the materials developed in this study. Capability of nano-size metastable particulates to increase the ductility of magnesium has been reported elsewhere [16, 17].

The work of fracture expresses the ability of each material to absorb energy up to fracture under tensile load and was computed using stress-strain diagram [7]. It reveals that nano-size oxide reinforced composites are distinctly superior when compared to unreinforced magnesium (see Table III) and significantly improved the fracture resistance of matrix. In essence, the results of tensile testing revealed that Mg/Al₂O₃ formulations are most suitable for strength based designs (higher yield strength when compared to magnesium and other composites in this study) while the Mg/ZrO₂ formulations appears to be more suitable for damage tolerant designs (higher work of fracture when compared to magnesium and other composites in this study) with good formability.

The results further revealed that addition of 1.1 volume percent of nano-size alumina particulates lead to an improvement in overall combination of mechanical properties that is not matched even by AZ91/SiC containing

much higher volume percentage of micron size SiC particulates (see Tables II and III). This also translates into even lighter weight and further enhanced specific mechanical properties (see Table III).

The meticulous study of uniaxially deformed fracture surfaces revealed the microstructural effects on tensile ductility and fracture properties of oxide dispersion strengthened pure magnesium. Typical brittle fracture surface (Fig. 2a) [7] with the presence of microscopically rough small steps has been seen in the case of Mg samples. However, fractography of dispersion strengthened composite samples revealed salient features such as: (a) ductile fracture of metal with void-sheet mechanism showing dimples [7]) (see Fig. 2b), (b) intergranular crack propagation (typical for hexagonal metal to improve its ductility [21]) (see Fig. 2c), and (c) branching of propagating crack at reinforcement particulates (typical way to improve ductility of metal with hexagonal crystal structure [18]) (see Fig. 2d).

Under the influence of far-field tensile load the fine microscopic voids including grain boundary ledges appeared and propagated by the void-sheet mechanism before coalescing to form dimples on the fracture surface. This is typical ductile nature of fracture mode that requires homogeneous deformation of matrix which is naturally restricted in hexagonal crystal structured magnesium by basal slip system [7, 42]. Activation of non-basal slip system is necessary to modify typical cleavage crack propagation to failure with homogeneous plastic deformation to failure in pure magnesium matrix and it is apparent in the cases of nano oxide dispersion strengthened magnesium. Presence of nanosize oxide reinforcement and refined microstructure is believed to initiate the activation of non-basal slip system in the developed composite materials as seen in Fig. 3(b). Activation of non-basal slip system in magnesium matrix due to the presence of reinforcement [19] and grain refinement [42] has been reported in open literature by other researchers. Again, presence of intergranular crack propagation (see Fig. 2c) and dissipation of stress concentration by branching the propagating crack tip (see Fig. 2d) in the fracture surfaces signifies improved plastic deformation in hexagonal crystal structured magnesium matrix. The fundamental principles behind the ability of fine oxide dispersoids in the brittle hexagonal metallic-matrix to enhance homogeneous plastic deformation [18, 21] have been already established and will not be discussed here. It is interesting to note that the fracture of the plastically deforming magnesium metal matrix was changed from complete cleavage mode to mixed mode of ductile and intergranular, dominated by formation, growth and coalescence of the microscopic voids with the activation of non-basal slip system in the presence of nano-size oxide particulates.

5. Conclusions

(1) Blend-press-sinter powder metallurgy technique coupled with hot extrusion can be used to synthesize Mg

based composites containing nano-size oxide particulates reinforcement e.g., Al_2O_3 , Y_2O_3 and ZrO_2 .

(2) Microstructural characterization shows reasonably uniform distribution of reinforcements with good matrix-reinforcement interfacial integrity. The presence of reinforcing particulates, irrespective of type, assisted in the significant grain refinement of magnesium matrix.

(3) The results of mechanical characterization revealed that the presence of the nano-size oxide particulates in magnesium matrix lead to significant improvement in hardness, 0.2%YS, UTS, ductility and work of fracture.

(4) Amongst the particulates type investigated, Al_2O_3 particulates were found to be most effective in increasing strength properties while the ZrO_2 particulates were most effective in increasing ductility and work of fracture.

(5) Fractography revealed that fracture behavior of the plastically deforming magnesium metal matrix was changed from complete cleavage mode to mixed mode of ductile and intergranular, dominated by formation, growth and coalescence of the microscopic voids with the activation of non-basal slip system in the presence of nano-size oxide particulates.

Acknowledgments

Authors wish to acknowledge NUS RP R-265-000-104-112 and NUSNNI for supporting this research effort. Thanks are also due to Ms Zhong Xiang Li for her help in FESEM and Quanta 3D studies.

References

1. A. BECK, in "Magnesium und seine Legierungen" (Springer-Verlag, Berlin, 1939).
2. R. FINK, in "Die-Casting Magnesium, Magnesium-Alloys and Technologies," edited by K. U. Kainer (Wiley-VCH Verlag GmbH & Co., Weinheim, Germany, 2003) p. 23.
3. C. AKEY and J. DAVIS, in "Magnesium: The Performance Material" (International Magnesium Association, Dearborn, MI, 1989) p. 1.
4. S. SCHUMANN and F. FRIEDRICH, in "Material Alloys and their Applications," edited by B. Mordike and K. Kainer, (Werkstoff-Informationsgesellschaft mbH, Wolfsburg, Germany, 1998) p. 3.
5. G. COLE, in "Magnesium into the Next Millennium" (International Magnesium Association, Rome, Italy, 1999) p. 21.
6. H. FRIEDRICH and S. SCHUMANN, in Magnesium 2000: Proceedings of the Israeli International Conference on Magnesium Science and Technology, edited by E. Aghion and D. Eliezer (Kavim Ltd., Beer-Sheva, Israel, 2000) p. 9.
7. R. E. REED-HILL, in "Physical Metallurgy Principles," 2nd edn. (NY, USA, D. Van Nostrand Company, 1964) p. 192, 267 and 725.
8. D. J. LLOYD, *Int. Mater. Rev.* **39**(1) (1994) 1.
9. D. M. LEE, B. K. SUH, B. G. KIM, J. S. LEE and C. H. LEE, *Mater. Sci. Tech.* **13** (1997) 590.
10. H. FERKEL and MORDIKE B. L., *Mater. Sci. Engng. A* **298** (2001) 193.
11. S. F. HASSAN and M. GUPTA, *Mater. Sci. Tech.* **19M** (2003) 253.
12. S. F. HASSAN and M. GUPTA, *J. Mater. Sci.* **37** (2002) 2467.
13. J. LLORCA, A. NEEDLEMAN and S. SURESH, *Acta. Metal. Materialia*, **39**(10) (1991) 2317.
14. A. R. VAIDYA and J. J. LEWANDOWSKI, *Mater. Sci. Engng. A* **220** (1996) 85.

15. R. UNVERRICHT, V. PEITZ, W. RIEHEMANN and H. FERKEL, in *Proceeding of Conference on Magnesium Alloys and Their Applications*, Germany, 1998, p. 327.
16. ALOK SINGH, M. NAKAMURA, M. WATANABE, A. KATO and A. P. TSAI, *Scripta Materialia* **49** (2003) 417.
17. A. G. GUY, in "Elements of Physical Metallurgy," 2nd edn. (USA, Addison-Wesley, 1967) p. 233.
18. GEORGE S. ANSELL, in "Physical Metallurgy," edited by R. W. Cahn (North-Holland Publishing Company, Netherlands, 1970) p. 1083.
19. P. PEREZ, G. GARCES and P. ADEVA, *Comp. Sci. Tech.* **64** (2004) 145.
20. S. F. HASSAN and M. GUPTA, *J Alloys Compd.* **345** (2002) 246.
21. WEI YANG and W. B. LEE, in "Mesoplasticity and its Applications" (Materials Research and Engineering, Springer-Verlag, Berlin, Germany, 1993) p. 361.
22. N. EUSTATHOPOULOS, M. G. NICHOLAS and B. DREVET, in "Wettability at High Temperatures" (Pregamon Materials Series, Elsevier, UK, 1999) vol. 3, p. 198.
23. J. D. GILCHRIST, in "Extraction Metallurgy," 3rd edn. (Pergamon Press, Great Britain, 1989) p. 148.
24. M. J. TAN and X. ZHANG, *Mater. Sci. Engng A* **244** (1998) 80.
25. P. G. SHEWMON, in "Transformation in Metals" (McGraw-Hill Book Company, NY, USA, 1969) p. 69.
26. B. Q. HAN and D. C. DUNAND, *Mater. Sci. Engng A* **277** (2000) 297.
27. R. M. GERMAN, in "Powder Metallurgy Science," 2nd edn (Metal Powder Industries Federation, Princeton, N.J, USA, 1994).
28. L. E. MURR, in "Interfacial Phenomena in Metals and Alloys" (Addison-Wesley, MA, USA, 1975) p. 28, 202 and 340.
29. J. NASER, W. RIEHEMANN and H. FERKEL, *Mater. Sci. Engng. A* **234** **236** (1997) 467.
30. ASM Metal Reference Book, 3rd edn., edited by Michael Baucio, (ASM International, Materials Park, USA, 1993) p. 145.
31. R. MORRELL, in "Handbook of Properties of Technical and Engineering Ceramics, Part 1: An Introduction for the Engineer and Designer" (Her Majesty's Stationary Office, England, 1985) p. 82 and 95.
32. Y. S. TOULOUKIAN, in "Thermophysical Properties of High Temperature Solid Materials" (Purdue University, 1967) p. 552.
33. M. F. ASHBY and D. R. H. JONES, in "Engineering Materials I" (Butterworth-Heinemann, Oxford, Boston, USA, 1996) p. 34 and 86.
34. M. GUPTA and T. S. SRIVATSAN, *J. Mater. Engng. Perfor.* **8**(4) (1999) 473.
35. F. WUA, J. ZHUA, Y. CHEN and G. ZHANG, *Mater. Sci. Engng. A* **277** (2000) 143.
36. H. JYNGE and K. MOTZFELDT, *Electrochimica Acta* **25** (1980) 139.
37. NICHOLAS J. GRANT, in "Dispersed Phase Strengthening" in "Strengthening of Metals" edited by Donald Peckner (Reinhold Publishing Corporation, USA, 1964) p. 163.
38. G. E. DIETER, in "Mechanical Metallurgy" (McGraw-Hill Book Corporation, Singapore, 2001) p. 329.
39. WILLIAM D. CALLISTER, JR., in "Materials Science and Engineering: An Introduction" (John Wiley & Sons, Inc., USA, 1985) p. 101.
40. C. H. CA' CERES and W. J. POOLE, *Mater. Sci. Engng A* **332** (2002) 311.
41. M. GUPTA and T.S. SRIVATSAN, *Mater. Lett.* **51** (2001) 255.
42. J. KOIKE, T. KOBAYASHI, T. MUKAI, H. WATANABE, M. SUZUKI, K. MARUYAMA and K. HIGASHI, *Acts Materialia* **51** (2003) 2055.

*Received 2 May
and accepted 5 July 2005*